Direction-of-Arrival Estimation using a Direct-Data Approach

This paper presents a direct-data (DD) counterpart to the covariance-based (CB) algorithm for direction-of-arrival (DOA) estimation. The proposed DD-DOA scheme provides reduced computational complexity as compared with other ESPRIT variations, filling in a theoretical gap not covered by previously presented schemes. A mean-squared error (MSE) analysis as well as computer simulations are provided allowing performance comparisons between DD-DOA and ESPRIT algorithms. The MSE performance is compared with the Cramer-Rao lower bound (CRLB) for one source. Results indicate that the proposed algorithm represents an efficient trade-off between computational complexity and final MSE as compared with standard ESPRIT schemes.

I. INTRODUCTION

Several modern wireless communication systems use spatial filtering for interference mitigation or source separation. Direction-of-arrival (DOA) estimation of the desired signal is a very useful technique for estimating optimal spatial filter coefficients [1]. First DOA estimation algorithms were based on nonparametric spectral estimation tools. Afterwards, new parametric maximum likelihood (ML) or eigenspace-based algorithms, such as the multiple signal classification (MUSIC) scheme [2], were proposed, reducing the associated computational load. Another popular family of DOA algorithms known as estimation of parameters via rotational invariance techniques (ESPRIT) [3] take advantage of redundancies within the receiving-array geometry to allow simplified implementations. The most recent proposal was the covariance-based (CB) DOA algorithm [4, 5], an ESPRIT variation with even lower computational complexity requiring the same geometrical constraints as before.

This article presents a direct-data (DD) alternative to the CB-DOA algorithm. The new scheme works with smaller data structures than ESPRIT, thus

resulting in a simpler DOA estimation technique, quite suitable for practical application scenarios such as radar systems [6]. This paper is organized as follows. Section II introduces the DOA problem and establishes the mathematical notation used throughout the paper; in Section III the DD-DOA algorithm is presented, where the associated convergence analysis is provided in Section IV; practical performance of the DD-DOA algorithm is verified in Section V, illustrating the positive characteristics of the proposed scheme with respect to final estimation error and overall computational complexity as compared with ESPRIT. Besides that, a comparison with the theoretical Cramer-Rao lower bound (CRLB) is also provided; Section VI closes the paper emphasizing its main contributions.

II. SYSTEM REPRESENTATION

Consider a wireless system comprising M signal sources and N receiving sensors. Assume that the receiving sensors may be grouped into pairs called doublets with a constant relative displacement Δ, as indicated in Fig. 1, constituting the so-called translational invariance constraint. One should keep in mind that a sensor may belong to two different doublets, as the initial or the terminal point of the displacement vector in each case. For instance, using the array of Fig. 1 with another choice for the doublets, sensor 2 may belong to a doublet with sensor 1, as the terminal point of the displacement vector, and to another doublet with sensor 3, as the initial point of the displacement vector.

Assume also that narrowband signals are transmitted, that the sources are coplanar, and that they all lie in the far-field of the receiving array. Let $s_m(t)$, for $0 \leq m \leq (M-1)$ represent the signal transmitted by the mth source at time t, and $z_{m,j}(t)$, for $0 \leq m \leq (M-1)$ and $0 \leq j \leq (N-1)$, denote the signal received at the jth sensor from the mth source. Then one may write that

$$z_{m,j}(t) = a_{m,j}s_m(t) + n_{m,j}(t) \qquad (1)$$

where $a_{m,j}$ and $n_{m,j}$ represent the directional gain and the additive white Gaussian noise (AWGN) component, respectively, in the jth receiving sensor for the impinging wave from the mth source.

The sensor pairing gives rise to two subarrays: one containing only the initial sensor and another with only the terminal sensor in each displacement vector. Let $x_{m,p}$ and $y_{m,p}$ denote the receiving signal in these two subarrays by the pth sensor, with $0 \leq p \leq (P-1)$, where P is the total number of doublets, for the mth signal source. Then P represents the number of sensors in each subarray, whereas N represents the total amount of sensors. One should notice that P and N must be in the range $(N/2) \leq P < N$. Therefore, for each subarray, one may rewrite (1)
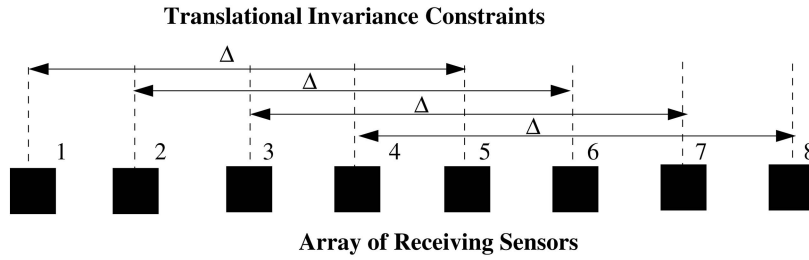
Translational Invariance Constraints

Fig. 1. Example of receiving array whose geometry satisfies translational invariance constraints.

as

$$x_{m,p}(t) = a_{m,p}s_m(t) + n_{m,p}(t) \qquad (2)$$

$$y_{m,p}(t) = a_{m,N-P+p}s_m(t) + n_{m,N-P+p}(t)$$

$$= a_{m,p}e^{j\omega\Delta\sin\theta_m/c}s_m(t) + n_{m,N-P+p}(t) \qquad (3)$$

where θ_m is the mth DOA angle, ω is the central frequency used for the transmission, and c represents the speed of light. The overall signal in each sensor is then represented by

$$x_p(t) = \sum_{m=0}^{M-1}(a_{m,p}s_m(t) + n_{m,p}(t)) \qquad (4)$$

$$y_p(t) = \sum_{m=0}^{M-1}(a_{m,p}e^{j\omega\Delta\sin\theta_m/c}s_m(t) + n_{m,p+P}(t)) \qquad (5)$$

for $0 \le p \le (P-1)$. Using a uniform time sampling $t = kT_s$, where T_s is the sampling period, the following discrete-time structures arise:

$$\mathbf{s}(k) = [s_0(k) \quad s_1(k)\cdots s_{M-1}(k)]^T \qquad (6)$$

$$\mathbf{x}(k) = [x_0(k) \quad x_1(k)\cdots x_{P-1}(k)]^T \qquad (7)$$

$$\mathbf{y}(k) = [y_0(k) \quad y_1(k)\cdots y_{P-1}(k)]^T \qquad (8)$$

$$\mathbf{z}(k) = [z_0(k) \quad z_1(k)\cdots z_{2P-1}(k)]^T \qquad (9)$$

$$\mathbf{n}_x(k) = \left[\sum_m n_{m,0}(k)\cdots\sum_m n_{m,P-1}(k)\right]^T \qquad (10)$$

$$\mathbf{n}_y(k) = \left[\sum_m n_{m,N-P+1}(k)\cdots\sum_m n_{m,N-1}(k)\right]^T \qquad (11)$$

$$\mathbf{A} = \begin{bmatrix} a_{0,0}(k) & a_{0,1}(k) & \cdots & a_{0,P-1}(k) \\ a_{1,0}(k) & a_{1,1}(k) & \cdots & a_{1,P-1}(k) \\ \vdots & \vdots & \ddots & \vdots \\ a_{M-1,0}(k) & a_{M-1,1}(k) & \cdots & a_{M-1,P-1}(k) \end{bmatrix} \qquad (12)$$

$$\boldsymbol{\Phi} = \mathrm{diag}([e^{j\omega\Delta\sin\theta_0/c}\cdots e^{j\omega\Delta\sin\theta_{M-1}/c}]). \qquad (13)$$

If a total of K vectors of samples (snapshots) are collected, one can define the overall structures

$$\mathbf{S} = [\mathbf{s}(0) \quad \mathbf{s}(1)\cdots\mathbf{s}(K-1)] \qquad (14)$$

$$\mathbf{X} = [\mathbf{x}(0) \quad \mathbf{x}(1)\cdots\mathbf{x}(K-1)] \qquad (15)$$

$$\mathbf{Y} = [\mathbf{y}(0) \quad \mathbf{y}(1)\cdots\mathbf{y}(K-1)] \qquad (16)$$

$$\mathbf{Z} = [\mathbf{z}(0) \quad \mathbf{z}(1)\cdots\mathbf{z}(K-1)] \qquad (17)$$

$$\mathbf{N}_X = [\mathbf{n}_x(0) \quad \mathbf{n}_x(1)\cdots\mathbf{n}_x(K-1)] \qquad (18)$$

$$\mathbf{N}_Y = [\mathbf{n}_y(0) \quad \mathbf{n}_y(1)\cdots\mathbf{n}_y(K-1)] \qquad (19)$$

allowing the following system description in matrix form:

$$\mathbf{X} = \mathbf{AS} + \mathbf{N}_X \qquad (20)$$

$$\mathbf{W} = \mathbf{X} + \mathbf{Y} = \mathbf{A}(\mathbf{I} + \boldsymbol{\Phi})\mathbf{S} + \mathbf{N}_X + \mathbf{N}_Y \qquad (21)$$

where $\mathbf{I}$ denotes the $M \times M$ identity matrix. One should note that $\mathbf{Z} = \begin{bmatrix}\mathbf{X}^T & \mathbf{Y}^T\end{bmatrix}$. The structure $\mathbf{B}$ is also defined such that

$$\mathbf{B} = \begin{bmatrix}\mathbf{X} \\ \mathbf{W}\end{bmatrix}. \qquad (22)$$

III. DIRECT-DATA-BASED DOA ESTIMATION

Assuming that $\boldsymbol{\Phi}$ has full rank and that the noise is both spatially as well as temporally white, one can prove that $\mathbf{X}$ and $\mathbf{W}$ span the same signal subspace. By performing a singular value decomposition (SVD) on $\mathbf{X}$,

$$\mathbf{X} = \mathbf{U}_X\boldsymbol{\Sigma}_X\mathbf{V}_X^H. \qquad (23)$$

One can relate the M largest singular values, as well as their associated left and right singular vectors [3], to the signal subspace. Let the diagonal matrix $\boldsymbol{\Sigma}_X$ be partitioned into two sections: $\boldsymbol{\Sigma}_{X,S}$, associated to signal-plus-noise components, containing the M largest singular values of $\boldsymbol{\Sigma}_X$, and $\boldsymbol{\Sigma}_{X,N}$, associated solely to noise components, containing the remaining singular values. One may form a new matrix $\boldsymbol{\Sigma}_{X,(S-N)}$ by subtracting the average of the diagonal entries of $\boldsymbol{\Sigma}_{X,N}$ from $\boldsymbol{\Sigma}_{X,S}$. Then one can define the following auxiliary structure that spans the signal subspace:

$$\mathbf{F} = \mathbf{U}_{X,S}\boldsymbol{\Sigma}_{X,(S-N)}^{1/2} \qquad (24)$$

with $\mathbf{U}_{X,S}$ comprising the first M columns of $\mathbf{U}_X$. Since the array manifold matrix $\mathbf{A}$ also spans the

signal subspace, there must be a full-rank matrix $\mathbf{T}_1$ such that

$$\mathbf{F} = \mathbf{AT}_1. \tag{25}$$

By defining $\mathbf{\Psi} = \mathbf{F}^{-1}\mathbf{W}$, from (22) and (25), one has that

$$\mathbf{\Psi} = \mathbf{T}_1^{-1}(\mathbf{I} + \mathbf{\Phi})\mathbf{T}_2 + \mathbf{F}^{-1}(\mathbf{N}_X + \mathbf{N}_Y). \tag{26}$$

In the noiseless case $\mathbf{N}_X = \mathbf{N}_Y = \mathbf{0}$ and $\mathbf{T}_2 = \mathbf{S}$, and then $\mathbf{\Phi}$ can be estimated from the result of an SVD on $\mathbf{\Psi}$. The same operation can also be performed in the general noisy case, by writing (26) as

$$\mathbf{\Psi} = \mathbf{T}_1^{-1}[(1 + \alpha)\mathbf{I} + \mathbf{\Phi}]\mathbf{T}_2 \tag{27}$$

with the parameter α embodying all effects from the noise structures $\mathbf{N}_X$ and $\mathbf{N}_Y$ projected on the signal subspace matrix $\mathbf{F}^{-1}$. In practice, α may reflect the uncertainty on the estimation of the signal subspace $\mathbf{U}_{X,S}$, and for that reason its value may be set as the estimated noise power scaled by a small constant. By performing an SVD on $\mathbf{\Psi}$, and subtracting the term $(1 + \alpha)\mathbf{I}$, the DD DOA estimates are determined as

$$\hat{\theta}_i = \arcsin\left(\frac{c}{j\omega\Delta}\ln(\hat{\phi}_i)\right), \qquad 0 \le i < M \tag{28}$$

where $\hat{\phi}_i$ is the ith diagonal entry of the estimated $\hat{\mathbf{\Phi}}$.

IV. THEORETICAL ANALYSIS FOR THE MEAN-SQUARED ERROR

Consider the mean-squared error (MSE) for the DOA parameter θ_i,

$$\mathrm{MSE}(\theta_i, \hat{\theta}_i) = E[|\Delta\theta_i|^2] = E[|\theta_i - \hat{\theta}_i|^2] \tag{29}$$

where $E[\cdot]$ represents the statistical mean. For $M = 2$ sources, based on the analysis performed in [7], the relation between $E[|\Delta\theta_i|^2]$ and $E[|\Delta\phi_i|^2]$ may be expressed as

$$E[|\Delta\theta_i|^2] = \left(\frac{1}{\omega_i\cos\hat{\theta}_i}\right)^2\frac{E[|\Delta\phi_i|^2]}{2}. \tag{30}$$

Consider that $\mathbf{r}_i$ are the eigenvectors of $\mathbf{\Psi}$, that is, $\mathbf{\Psi}\mathbf{r}_i = (1 + \alpha + \phi_i)\mathbf{r}_i$. For the variables $\mathbf{\Delta\Psi}$ and $\Delta\phi_i$, the following relation holds,

$$\mathbf{\Delta\Psi}\mathbf{r}_i = \Delta\phi_i\mathbf{r}_i. \tag{31}$$

Hence, a first-order approximation for $\Delta\phi_i$ is given by

$$\Delta\phi_i \approx \mathbf{r}_i^H\mathbf{\Delta\Psi}\mathbf{r}_i. \tag{32}$$

One then considers the auxiliary structure $\mathbf{B}$ and the associated matrix $\mathbf{V}_B$ comprising all eigenvectors $\mathbf{v}_i$ of $\mathbf{R}_B = (1/\sqrt{K})\mathbf{BB}^H$ in a columnwise manner. By defining the $P \times 2P$ data-selection matrices $\mathbf{J}_{X,2P}$ and $\mathbf{J}_{Y,2P}$ such that

$$\mathbf{J}_{X,2P} = [\mathbf{I} \quad \mathbf{0}] \tag{33}$$

$$\mathbf{J}_{Y,2P} = [\mathbf{0} \quad \mathbf{I}] \tag{34}$$

where $\mathbf{I}$ is a $P \times P$ identity matrix, whereas $\mathbf{0}$ is a $P \times P$ matrix containing only zeros. We may partition $\mathbf{V}_B$ in such a way that $\mathbf{V}_X = \mathbf{J}_{X,2P}\mathbf{V}_B$ and $\mathbf{V}_W = \mathbf{J}_{Y,2P}\mathbf{V}_B$.

Based on the definition of $\mathbf{\Psi}$, one assumes that

$$\mathbf{\Psi}\mathbf{V}_X = \mathbf{V}_W \tag{35}$$

and we may then write

$$(\mathbf{\Psi} + \mathbf{\Delta\Psi})(\mathbf{V}_X + \mathbf{\Delta V}_X) = \mathbf{V}_W + \mathbf{\Delta V}_W. \tag{36}$$

Therefore, using (35) and considering $\mathbf{\Delta\Psi}\mathbf{\Delta V}_X \approx \mathbf{0}$, one gets

$$\mathbf{\Delta\Psi} = (\mathbf{\Delta V}_W - \mathbf{\Psi}\mathbf{\Delta V}_X)\mathbf{V}_X^+ \tag{37}$$

where $\mathbf{V}_X^+$ is the pseudoinverse of $\mathbf{V}_X$. Combining (32) and (37), and observing that $\mathbf{r}_i$ are the eigenvectors of $\mathbf{\Psi}$, one has that

$$\Delta\phi_i = \mathbf{r}_i^H(\mathbf{\Delta V}_W - (1 + \alpha + \phi_i)\mathbf{\Delta V}_X)\mathbf{V}_X^+\mathbf{r}_i \tag{38}$$

which may be expressed as

$$\Delta\phi_i = \mathbf{r}_i^H\mathbf{C}_i\mathbf{\Delta V}_B\mathbf{V}_X^+\mathbf{r}_i \tag{39}$$

where $\mathbf{C}_i = (\mathbf{J}_{Y,2P} - (1 + \alpha + \phi_i)\mathbf{J}_{X,2P})$. Therefore, $E[|\Delta\phi_i|^2]$ may be written as

$$E[|\Delta\phi_i|^2] = \mathbf{r}_i^H(\mathbf{V}_X^+)^H E[\mathbf{\Delta V}_B^H\mathbf{C}_i^H\mathbf{r}_i\mathbf{r}_i^H\mathbf{C}_i\mathbf{\Delta V}_B]\mathbf{V}_X^+\mathbf{r}_i. \tag{40}$$

By defining $\mathbf{\Delta v}_i$ as the estimation error for each eigenvector $\mathbf{v}_i$ of $\mathbf{BB}^H$, one has that

$$E[|\Delta\phi_i|^2] = \mathbf{r}_i^H(\mathbf{V}_X^+)^H\left(\sum_{j=1}^{M}|\mathbf{r}_i|^2\right)\mathbf{C}_i^H\mathbf{R}_{\Delta v}\mathbf{C}_i\mathbf{V}_X^+\mathbf{r}_i \tag{41}$$

with [7]

$$\mathbf{R}_{\Delta v} = E[\mathbf{\Delta v}_i\mathbf{\Delta v}_j^H] = \frac{\sigma_i}{N}\sum_{k=1,k\ne i}\frac{\sigma_i}{(\sigma_k - \sigma_i)^2}\mathbf{v}_k\mathbf{v}_k^H\delta(i - j) \tag{42}$$

where δ stands for the Kronecker impulse and σ_i^2 denotes an eigenvalue of $\mathbf{\Psi}$. Therefore, (41) may be rewritten as

$$E[|\Delta\phi_i|^2] = \mathbf{r}_i^H(\mathbf{V}_X^+)^H\left(\sum_{j=1}^{M}|\mathbf{r}_i|^2\mathbf{C}_i^H\frac{\sigma_i}{N}\sum_{k=1,k\ne i}\frac{\sigma_i}{(\sigma_k - \sigma_i)^2}\right.$$
$$\left. \times\mathbf{v}_k\mathbf{v}_k^H\delta(i - j)\mathbf{C}_i\right)\mathbf{V}_X^+\mathbf{r}_i \tag{43}$$

which can be plugged into (30) to obtain an expression for $E[|\Delta\theta_i|^2]$. The resulting expression is quite similar to the MSE expression for the ESPRIT algorithm, with the main differences lying on the definition of $\mathbf{\Delta v}_i$, which is associated to the eigenvectors of $(1/\sqrt{K})\mathbf{XX}^H$ for the ESPRIT

TABLE I
Short Descriptions of the TLS Implementation of ESPRIT and
DD-DOA Algorithm

TLS-ESPRIT	DD-DOA
$[\mathbf{U}, \mathbf{\Sigma}, \mathbf{V}^H] = \text{SVD}(\mathbf{Z})$	$\mathbf{X} = \mathbf{J}_{X,2P}\mathbf{Z}$
$\mathbf{U}_X = \mathbf{J}_{X,2P}\mathbf{U}$	$\mathbf{W} = (\mathbf{J}_{X,2P} + \mathbf{J}_{Y,2P})\mathbf{Z}$
$\mathbf{U}_Y = \mathbf{J}_{Y,2P}\mathbf{U}$	$[\mathbf{U}_X, \mathbf{\Sigma}_X, \mathbf{V}_X^H] = \text{SVD}(\mathbf{X})$
$\mathbf{U}_a = \begin{bmatrix} \mathbf{U}_X^* \\ \mathbf{U}_Y^* \end{bmatrix} [\mathbf{U}_X \quad \mathbf{U}_Y]$	$\mathbf{F}^{-1} = \mathbf{\Sigma}_{X,(S-N)}^{-1/2}\mathbf{U}_{X,S}^H$
$[\mathbf{E}, \mathbf{\Lambda}] = \text{EVD}(\mathbf{U}_a)$	$[\mathbf{T}_1, (1+\alpha)\mathbf{I} + \hat{\mathbf{\Phi}}, \mathbf{T}_2] = \text{SVD}(\mathbf{F}^{-1}\mathbf{W})$
$\mathbf{E}_{12} = \mathbf{J}_{X,2M}\mathbf{E}\mathbf{J}_{Y,2M}^T$	
$\mathbf{E}_{22} = \mathbf{J}_{Y,2M}\mathbf{E}\mathbf{J}_{Y,2M}^T$	
$\mathbf{\Psi} = -\mathbf{E}_{12}^{-1}\mathbf{E}_{22}$	
$[\mathbf{T}_1, \hat{\mathbf{\Phi}}] = \text{EVD}(\mathbf{\Psi})$	

TABLE II
Number of Flops and Matrix Operations Required by TLS
Implementation of ESPRIT and DD-DOA Algorithm

Operation [8]	TLS-ESPRIT		DD-DOA	
	#	Flops	#	Flops
SVD $\mathcal{O}(2mn^2)$	1	$4PK^2$	2	$2PK^2 + 2MK^2$
EVD $\mathcal{O}(25n^3)$	1	$200P^3$	—	—
Hermit. EVD $\mathcal{O}(n^2)$	1	P^2	—	—
Full Inverse $\mathcal{O}(n^3)$	1	P^3	—	—
Multiplic. $\mathcal{O}(mnk)$	5	$5P^3$	2	$P^2K + M^2P$
Total		$4PK^2 + 206P^3$ $+P^2$		$2PK^2 + 2MK^2$ $+P^2K + M^2P$

algorithm, and on the definition of $\mathbf{C}_i$, which becomes $\mathbf{C}_i^{\text{ESPRIT}} = (1 - \phi_i^*)\mathbf{J}_{X,2P}$ for the ESPRIT algorithm [7].

The MSE analysis above is based on the eigenvalues of the received signals. As the DD-DOA algorithm operates on the corresponding singular values, which are constrained to be real numbers, the imaginary part of each ϕ_i in (28) must be estimated from its real part, forcing a unitary norm. This procedure introduces a cumulative error component onto the DD-DOA algorithm which is not present in ESPRIT.

V. PERFORMANCE ASSESSMENT

A. Computational Complexity

In order to compare the computational complexity of DD-DOA to the TLS (total least-squares) implementation of the standard method ESPRIT [3], Table I summarizes the main operations performed by each algorithm, where $\mathbf{J}_{X,2M}$ and $\mathbf{J}_{Y,2M}$ are similar structures to the selection matrices defined by (33) and (34), respectively, also comprising an identity and a null matrix. For matrices $\mathbf{J}_{X,2M}$ and $\mathbf{J}_{Y,2M}$, however, both the null submatrix $\mathbf{0}$ and the identity submatrix $\mathbf{I}$ have dimensions $M \times M$. One may notice that the DD-DOA algorithm uses the data structures $\mathbf{X}$ and $\mathbf{W} = (\mathbf{X} + \mathbf{Y})$, not requiring $\mathbf{Y}$ explicitly. Note also

that $\mathbf{F}^{-1}$ is directly computed, requiring the lower complexity operation of inverting a diagonal matrix.

One observes, from Table I, that the ESPRIT algorithm requires:

1) 1 SVD for an $N \times K$ matrix;
2) 2 EVD (eigenvalue/eigenvector decomposition) (1 for a $P \times P$ non-Hermitian matrix, and 1 for a $P \times P$ Hermitian matrix);
3) 1 full inversion for a $P \times P$ matrix;
4) 5 multiplications, all of them between $P \times P$ matrices.

On the other hand, the DD-DOA algorithm requires:

1) 2 SVD (1 for a $P \times P$ matrix and one for an $M \times K$ matrix);
2) 2 multiplications (1 between a $P \times P$ matrix and a $P \times K$ matrix, and 1 between an $M \times M$ matrix and an $M \times P$ matrix).

A more detailed comparison of the two algorithms is then performed in Table II. Since the parameter K, which represents the number of snapshots, is usually the largest variable, the K^2 terms tend to dominate the overall burden for each algorithm. In such a case, as the number of samples K gets larger, the DD-DOA algorithm represents computational savings on the order of $(M + P)/2P$ in comparison with TLS-ESPRIT.

B. Computer Simulations

1) *Comparison to ESPRIT*: Some experiments are included to compare the performance of DD-DOA algorithm with the standard TLS version of the ESPRIT algorithm. A signal from each source was randomly generated from a Gaussian distribution and simulations were performed for $M = 2$ sources located at angles $\theta_1 = -8°$ and $\theta_2 = 9°$. Algorithm performance was assessed according to the total MSE ξ, defined as

$$\xi = \frac{1}{M}\sum_{i=0}^{M-1} E[|\Delta\theta_i|^2] \qquad (44)$$

where the statistical mean was estimated by averaging the squared error over 500 independent Monte Carlo measurements of the squared error. The total MSE was determined for distinct values of the signal-to-noise ratio (SNRs) measured at the receiver input over 6000 snapshots. The simulated MSE measurements also aim to validate the theoretical MSE analysis presented in Section IV. Theoretical as well as simulated curves are presented in Fig. 2 for $M = 2$ sources and $P = 14$ sensors. The results for $P = 14$ receiving sensors for both algorithms are shown in Fig. 2, which indicates a higher ξ for the DD-DOA algorithm, mainly due to the estimation of the imaginary part of $\hat{\phi}_i$ from its real part. Nevertheless, for such a scenario, the simulated DD-DOA requires
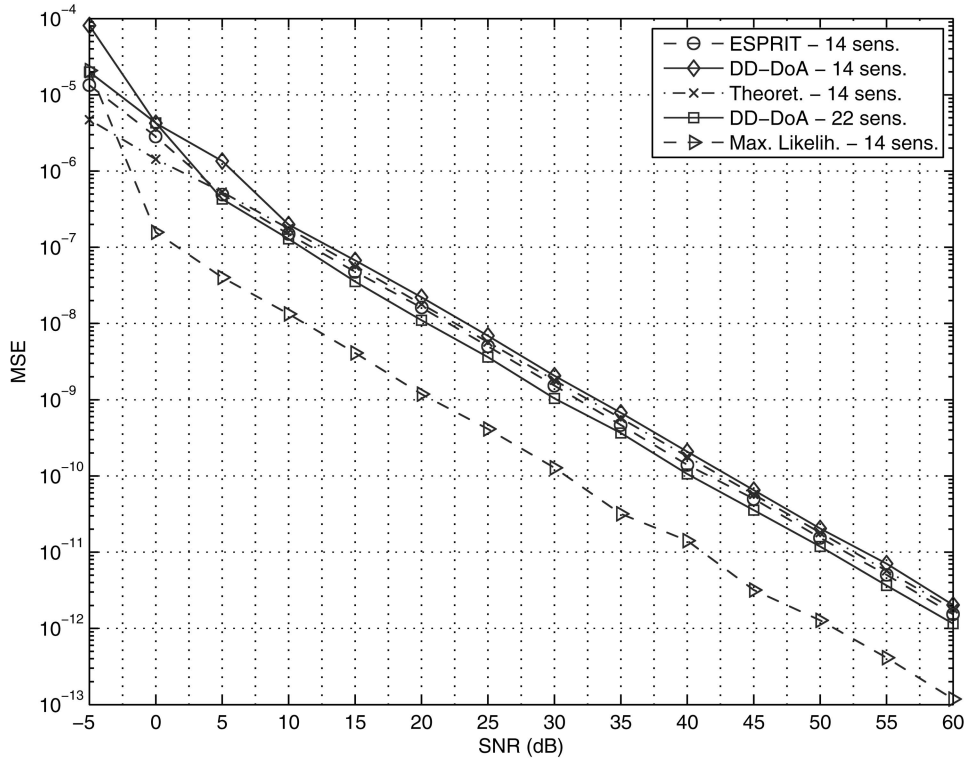
Fig. 2.   Total MSE comparison of theoretical (as determined in (30)) and simulated DOA estimates with $M = 2$ sources for ESPRIT (with $P = 14$ sensors), DD-DOA (with $P = 14$ and $P = 26$) and ML (with $M = 2$ and $P = 14$) algorithms.

around 42% less FLOPs than ESPRIT. Practical perfomance achieved by the DD-DOA algorithm corroborates theoretical analyses represented by (30) and (43), also shown in Fig. 2 for $P = 14$. As mentioned in Section VA, when using $M = 2$ sources, the computational complexity associated to the ESPRIT algorithm with $P = 14$ receiving sensors is about the same as of the DD-DOA algorithm with $P = 26$ receiving sensors. Therefore, the total MSE for the DD-DOA with $P = 26$ receiving sensors is also shown in Fig. 2, indicating a superior performance of this algorithm, for the same computational burden, as compared with the ESPRIT algorithm.

Another comparison performed in Fig. 2 is related to the ML estimator, defined by [1] as

$$\psi_{\mathrm{ML}} = \arg\min_{\mathbf{A}} \left\{ \det[\mathbf{P}_A \mathbf{R}_z \mathbf{P}_A + \frac{1}{N} \mathrm{tr}(\mathbf{P}_A^{\perp} \mathbf{R}_z) \mathbf{P}_A^{\perp}] \right\}$$

(45)

where $\mathbf{P}_A$ denotes the projection matrix onto the columns of the extended array manifold $\mathbf{A}_{\mathrm{ext}}$, that is,

$$\mathbf{P}_A = \mathbf{A}_{\mathrm{ext}}(\mathbf{A}_{\mathrm{ext}}^H \mathbf{A}_{\mathrm{ext}})\mathbf{A}_{\mathrm{ext}}^H,$$

(46)

where

$$\mathbf{A}_{\mathrm{ext}} = \begin{bmatrix} \mathbf{A} \\ \mathbf{A}\mathbf{\Phi} \end{bmatrix}.$$

(47)

Besides that, $\mathbf{R}_z = (1/\sqrt{K})\mathbf{Z}\mathbf{Z}^H$ is the estimated correlation for $\mathbf{z}(k)$. The ML estimator presents a lower MSE than both the proposed DD-DOA and

the standard ESPRIT algorithms for the whole range of simulated MSEs. On the other hand, ML requires much more complex operations than both DD-DOA and ESPRIT algorithms. At around −5 dB the performance of all the algorithms becomes severely degraded, especially ML and DD-DOA with 14 sensors.

2) *Cramer-Rao Lower Bound*:   The Cramer-Rao lower bound (CRLB) represents the theoretical limit for the variance of an unbiased estimator. In order to assess the MSE performance of the proposed estimator in comparison to the CRLB, a simplified expression for the CRLB for $M = 1$ transmitting source was used [1]

$$\mathrm{CRLB}(\theta, \hat{\theta}) = \frac{6}{P^3 K (\mathrm{SNR})}$$

(48)

where a large number K of data snapshots is assumed. Using a simulation scenario comprised of $M = 1$ source, $P = 8$ receiving sensors, and $K = 18000$ snapshots, the resulting MSE resulting from (48) and the simulated MSE for the DD-DOA algorithm is seen in Fig. 3 for distinct SNR values, reaching the MSE threshold region near the lower values of SNR. This figure shows that the DD-DOA performance is around twice the CRLB value for SNR values above the threshold region, which is similar to the results achieved by the ESPRIT and the CB-DOA algorithms included in [4].

Performance of the ML estimator is also shown for one source in Fig. 3, presenting smaller MSE in
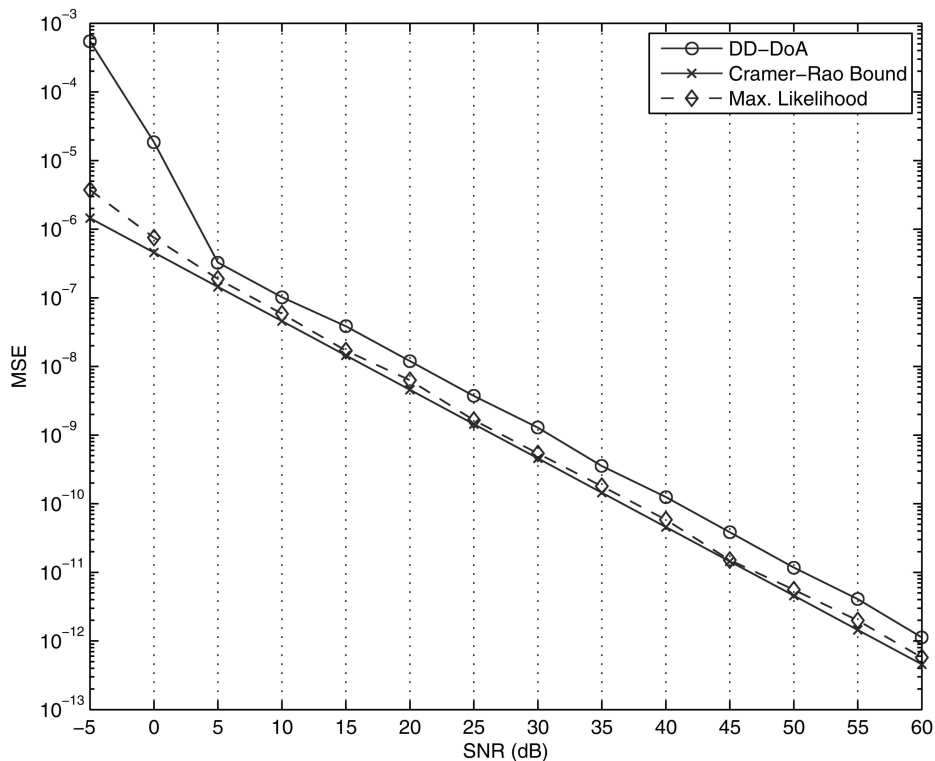
Fig. 3. CRLB and total MSE for both ML and DD-DOA, for $M = 1$ source, $P = 8$ receiving sensors, and $K = 18000$ data snapshots.

comparison with the proposed DD-DOA algorithms. Neverthless, regarding computational complexity, both DD-DOA and ESPRIT algorithms are much less computationally complex than the solution search for the ML estimator.

VI. CONCLUSIONS

In this article, the parametric DD algorithm for DOA estimation is presented as a low computational complexity alternative to the SVD-based version of ESPRIT. Both theoretical analysis and computer simulations indicate that the proposed DD-DOA algorithm presents lower MSE for a similar computational complexity as compared with the standard ESPRIT algorithm or lower computational complexity for a similar MSE performance.

TADEU N. FERREIRA
SERGIO L. NETTO
PAULO S. R. DINIZ
Electrical Engineering Program
Federal University of Rio de Janeiro
PO Box 68504
Rio de Janeiro
Brazil
E-mail: (tadeu.n.ferreira@gmail.com)

REFERENCES

[1]   Van Trees, H.
         Detection, Estimation and Modulation Theory, Part IV: Optimum Array Processing.
         Hoboken, NJ: Wiley, 2002.

[2]   Schmidt, R. O.
         Multiple emitter location and signal parameter estimation.
         In *Proceedings of the RADC Spectral Estimation Workshop*, 1979, 243–258.

[3]   Roy, R. and Kailath, T.
         ESPRIT—Estimation of parameters via rotational invariance techniques.
         IEEE Transactions on Acoustics, Speech, and Signal Processing, **37**, 7 (July 1989), 984–995.

[4]   Ferreira, T., Netto, S. L., and Diniz, P. S. R.
         Low complexity covariance-based DOA estimation algorithm.
         In *Proceedings of the 15th European Signal Processing Conference*, Poznan, Poland, Sept. 2007, 100–104.

[5]   Zoltowski, M.
         Novel techniques for estimation of array signal parameters based on matrix pencils, subspace rotations and total least-squares.
         In *Proceedings of the IEEE ICASSP*, Seattle, WA, May 1998, 2861–2864.

[6]   Athley, F., Engdahl, C., and Sunnergren, P.
         On radar detection and direction finding using sparse arrays.
         IEEE Transactions on Aerospace and Electronics Systems, **43**, 4 (Oct. 2007), 1319–1333.

[7]   Rao, B. D. and Hari, K. V. S.
         Performance analysis of ESPRIT and TAM in determining the direction of arrival of plane waves in noise.
         IEEE Transactions on Acoustics, Speech, and Signal Processing, **37**, 12 (Dec. 1989), 1990–1995.

[8]   Golub, G. and Van Loan, C.
         Matrix Computations (3rd ed.).
         Baltimore, MD: The Johns Hopkins University Press, 1996.